

Research on the Influence Law of Vibration on Grade G Cement

Manli Niu *, Xinyuan Wu

School of Mechanical Engineering, Sichuan University of Science & Engineering, Zigong, China

* Corresponding Author: Manli Niu

ABSTRACT

The paper investigates the effect of vibration on compressive strength and cementitious strength of cement stone through experiments, analyzes the effect of different vibration parameters on the macroscopic mechanical properties of cement, and microscopically, it is observed by electron microscope to verify the effect of vibration on cement stone to improve the internal structure of cement stone, and the experimental results show that vibration is able to significantly improve the compressive strength and cementitious strength of cement stone. Within a certain range, with the increase of vibration frequency and time, the compressive strength gradually increases, while the cement strength shows a trend of increasing first and then stabilizing. It is found that vibration can promote a more uniform distribution of cement particles, reduce the number and size of pores, vibration 20Hz, 40Hz and 60Hz compared with the porosity of static cement reduced by 23.14%, 39.72% and 50.79%, improving the compactness of cement stone. Guidelines are provided for the selection of optimal vibration parameters for vibratory cementing tool operations.

KEYWORDS

Vibration; Grade G Cement; Mercury Pressure Method.

1. INTRODUCTION

In cementing operation, the strength performance of cement stone is an important index to evaluate the cementing quality of a well, which directly affects the long-term cementing quality of wellbore[1-3]. As early as in the 1980s, Cooke et al. proposed the mechanical vibration casing technology to improve the quality of single-well cementing and effectively solve the problem of cement paste cementing weight loss[4]. In-depth experiments on the effect of mechanical vibration on the performance of drilling fluid have been conducted, and it is found that vibration can improve the rheological properties of drilling fluid, increase the strength of cement stone, and prevent the annulus from running out of gas, meanwhile, the operation of mechanical vibration is simple and convenient, and the tools and equipments can be reused at a low cost, so it can be used in all the cementing operations. Meanwhile, mechanical vibration operation is simple and easy to realize, tools and equipments can be reused with low cost, which is beneficial to all cementing processes, so mechanical vibration cementing technology is regarded as a new technology to improve the quality of cementing[5-7].

At present, the main research institutes and production units in China mainly focus on the development and design of vibratory cementing tools and equipments[8-11], with less research on the mechanical properties of cement, especially on the effect of vibration on the microscopic morphology of cement, porosity, pore size distribution and so on. Experiments on the effect of vibration on the properties of cement stone.

2. EXPERIMENTS ON THE EFFECT OF VIBRATION ON THE PROPERTIES OF CEMENT STONES

2.1. Experimental Equipment

In order to effectively evaluate the effect of mechanical vibration on the mechanical properties of cement stones, the following experimental system was used in this experiment. The system is simple in design, easy to assemble and low cost, and is able to simulate the action of vibration in the cement paste during the setting stage through indoor experiments. Through this system, the best vibration parameters suitable for improving the strength of cement stone can be selected, and the applicability of vibration to different cement paste systems can be analyzed, so as to objectively and realistically evaluate the effect of vibration on the quality of cementing.

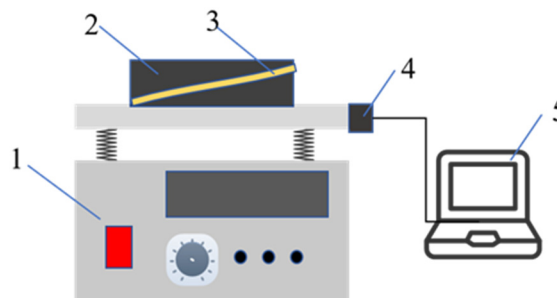


Figure 1. Schematic diagram of experimental apparatus

Figure Note 1-Shaker 2-Mold 3-Nylon strap 4-Sensor 5-Computer

The experiment is shown in Fig. 1. The experimental system consists of three separate modules: frequency and amplitude adjustable shaker, vibration measuring instrument and mold. During the experiment, the simple harmonic load of the shaker is used to simulate the effect of the vibrating tool on the cement paste. The parameters of the equipment are shown in Table 1, and the maximum load capacity of the shaker is 10 kg. The vibration parameters of the shaker are determined with reference to the analysis of the vibration propagation law in Chapter III. The vibration table can provide a vibration frequency range of 0~60Hz, and the platform size is 250mm×250mm, which can accommodate the cement mold and basically meet the needs of simulated vibration conditions. The vibration frequency is adjusted by a knob and the amplitude is measured by an acceleration sensor, which is fixed to the vibration table by a magnetic base.

Table 1. Vibration table device technical parameters

Countertop Size(mm)	Direction of vibration	Maximum test load(kg)	amplitude(mm)	FM range
250×250	vertical	10	0~2mm	0~60Hz

2.2. Experimental Program Design

The purpose of this experiment is to study the effect of vibration parameters on the compressive strength and cementitious strength and microstructure of G grade cement by loading simple harmonic loads with different parameters on G grade cement during the Hou setting period, and to find out the law of vibration parameters and mechanical properties and structural changes, and the experimental program will be designed as follows.

1)experimental material

The cement used in the experiment is Sichuan Jiahua G grade oil well cement, and its main components are shown in Table 2.

Table 2. Main Components of Sichuan Jiahua G-grade Cement

Component	tricalcium aluminum oxide	free calcium oxide	Tetracalcium iron aluminate	dicalcium silicate	tricalcium silicate
Content/%	1-2	≤0.5	15-16	14-19	62-67

2) experimental condition

In order to compare the effects of different vibration parameters on the compressive strength and cementitious strength of grade G cement, the vibration frequency range of 0~40Hz, vibration time range of 0~30min, and vibration amplitude of 1mm simple harmonic load were selected.

3) Experimental Flow

Before preparing the cement slurry, the cement should be sieved using an 850- μ m metal sieve to remove larger particles and ensure the homogeneity and quality of the cement. According to the GB/T 10238-2015 standard, weigh the cement and mixing water accurately according to the ratio of water-cement ratio of 0.44. Start the mixing equipment, set the rotational speed at 4000 r/min, and add the cement sample uniformly within 15 seconds. After the cement was added, the mixing was continued at 4000 r/min for 15 seconds, and then the speed was increased to 11000 r/min and the mixing was continued for 35 seconds to ensure that the cement slurry was well mixed.

After preparation, the cement slurry was poured into pre-prepared cylindrical molds and buttered triplex molds to avoid adhesion of the cement slurry to the surface of the molds.

4) data processing

A total of 3 cement stone samples were obtained from each set of data, referring to the principle of laboratory data screening, the difference between the maximum and minimum values and the median value, if the ratio of the difference to the median value is more than 15%, the maximum or minimum value will be rounded off, and the remaining data will be averaged again, and if it doesn't comply with it, then the experiment will be carried out again, until it complies with the principle.

2.3. Experimental Results

Cement paste was prepared according to the above steps and the specific pattern of influence of vibration parameters on the strength of cementite was investigated. Since the vibration frequency and vibration time of the vibration tool were set by software, a one-way analysis of vibration frequency and vibration time was carried out. In the experiment, the blank control group was left to stand for 30 minutes, while the vibration group was subjected to high-temperature curing after 30 minutes of vibration, followed by demolding and placing into water at a temperature of 27°C for 40 minutes, and then tested for its compressive strength by means of a press .

As can be seen in Fig. 2, the compressive strength of cementite gradually increased with the increase of vibration frequency. The fastest increase in the strength of the cement stone was found within 0-20 Hz, while the increase gradually slowed down within 20-60 Hz and between 60 Hz, although the strength was still increasing. At lower frequencies, the excitation force of the vibration tool is small, and the propagation distance of the vibration wave and its effect on the cement stone are weak; while when the vibration frequency increases, the increase in the strength of the cement stone becomes slow, although the strength still increases. Therefore, combining the propagation law of vibration wave and the effect of vibration frequency on the performance of cement stone, it is recommended to control the vibration frequency in the range of 20~40Hz to realize the best vibration effect.

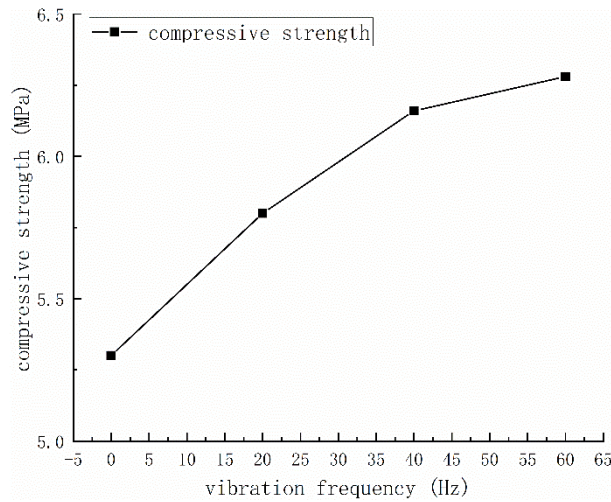


Figure 2. Variation of Compressive Strength of Cement Stone with Vibration Frequency

It can be seen from Fig. 3 that the compressive strength of the cement stone continued to increase with the increase in vibration time up to 20 minutes. In the vibration time however, when the vibration time is increased to 30 minutes, the increase in compressive strength starts to decrease. This is because the cement paste undergoes hydration reaction at the same time during the vibration process, and with the passage of time, the cement paste system gradually tends to be stabilized, and further increase in the vibration time will not significantly improve the compressive strength of cement. Therefore, in practice, it is recommended that the vibration tool should be used for more than 10 minutes to improve the mechanical properties of cement.

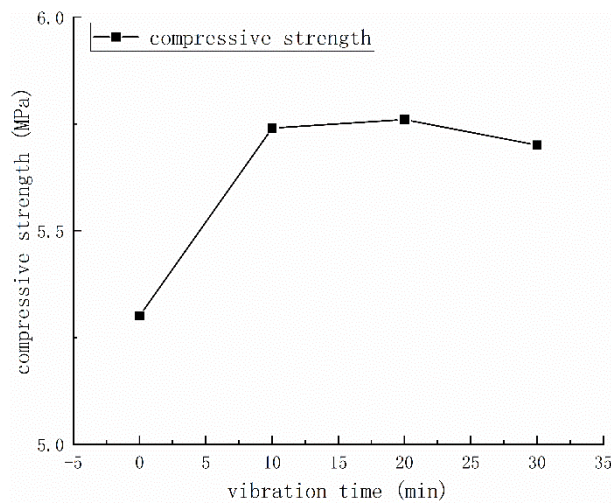


Figure 3. Variation of Compressive Strength of Cement Stone with Vibration Duration

As the experimental operation of cement bond strength refers to the compressive strength experiment, the cement bond strength is generally measured using the press-out method [12] and the tensile method[13,14], in accordance with the above steps to prepare the cement paste, the study of the vibration parameters of the first interface strength of cement stone specific influence on the law of the cement bond strength test schematic diagram as shown in the experimental steps are as follows: (1) the prepared cement paste is poured into the cylindrical molds and assembly (2) Fix the mold on the vibration table and load it according to the designed vibration parameters, put the mold into the designed maintenance conditions for a certain period of time and then take it out; (3) Pry open the upper and lower sealing end caps, use the press to press it out and record the pressure shown by the press when the interface is destroyed; (4) Convert the interface failure pressure into the interfacial cementation strength.

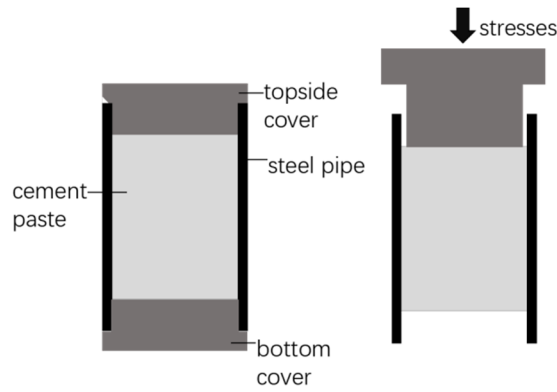


Figure 4. Schematic Diagram of Cementing Strength Test

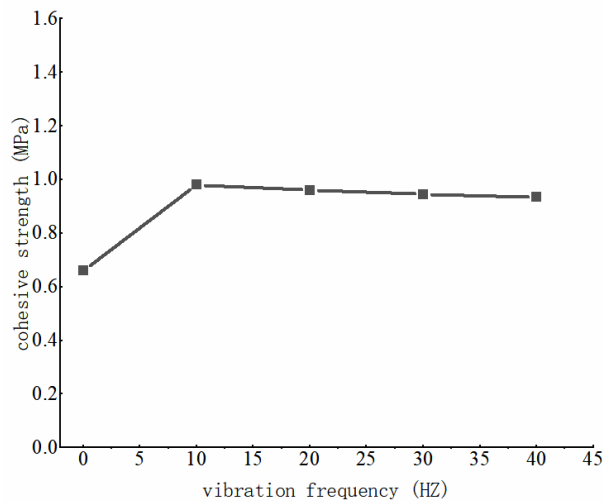


Figure 5. The Effect of Vibration Frequency on Cement Bonding Strength

Figure 5 can be obtained, with the increase in vibration frequency, the cement bond strength first increased and then slowly decreased, in the vibration frequency of 10Hz, making the maximum increase in the bond strength of 48.4%, the vibration frequency of more than 10Hz, the bond strength is basically stabilized, with the increase in frequency, the increase in the bond strength is slightly reduced, with the vibration frequency of 10Hz compared to the reduction of 2.04%, 3.57%, and 4.48%, which is different from the vibration effect on the compressive strength law. and 4.48%, which is different from the vibration effect law on compressive strength.

This shows that when considering the vibration parameters of the vibration tool, it is necessary to take into account the vibration frequency of the impact on the cement stone and the propagation law of the vibration wave, in the low-frequency vibration (0~20Hz), the cement compressive and cementitious strength increases, but the tool produces a smaller excitation force, although the propagation distance is far but the amplitude response is smaller; in the intermediate frequency of vibration (20~40Hz), the compressive strength of the cement increases, although the cementitious strength is somewhat reduced, but the amplitude is small, the vibration wave propagation distance is also relatively far, the amplitude response value is also relatively obvious; in the higher frequency vibration (40Hz-60Hz), although the compressive strength increases, but the cement strength is reduced, the vibration wave propagation distance is also rapidly reduced. It is thus believed that controlling the vibration frequency of the vibrating tool in the mid-frequency range will make the vibration of the vibrating tool more effective.

3. EFFECT OF VIBRATION ON THE MICROSTRUCTURE OF CEMENT

Combined with the microscopic experimental specimens prepared by the vibration scheme of class G cement, the corresponding microscopic experimental design scheme is designed as shown in Table 3, which is mainly to study the effect of different vibration frequencies on the microstructure of cement, with reference to the vibration wave propagation law in Chapter 3 and the experiments of the effect of different vibration frequencies on the mechanical properties of cement, to formulate the following experimental scheme, in which the NMR method needs to be combined with the mercuric compression to achieve the aperture distribution of the cementite Characterization.

Table 3. Microscopic Experimental Plan

methodologies	vibration frequency/Hz	vibration time/min	amplitude of vibration/mm
Electron microscope SEM analysis	0, 20, 40		
mercuric pressure	0, 20	30min	1mm
low-field nuclear magnetic resonance (NMR)	0, 40, 60		

3.1. Electron Microscope SEM Analysis

Fig. 6 shows the typical morphology of SEM of G-grade cement stone under different magnifications of control group and experimental group loaded under different vibration frequency conditions.

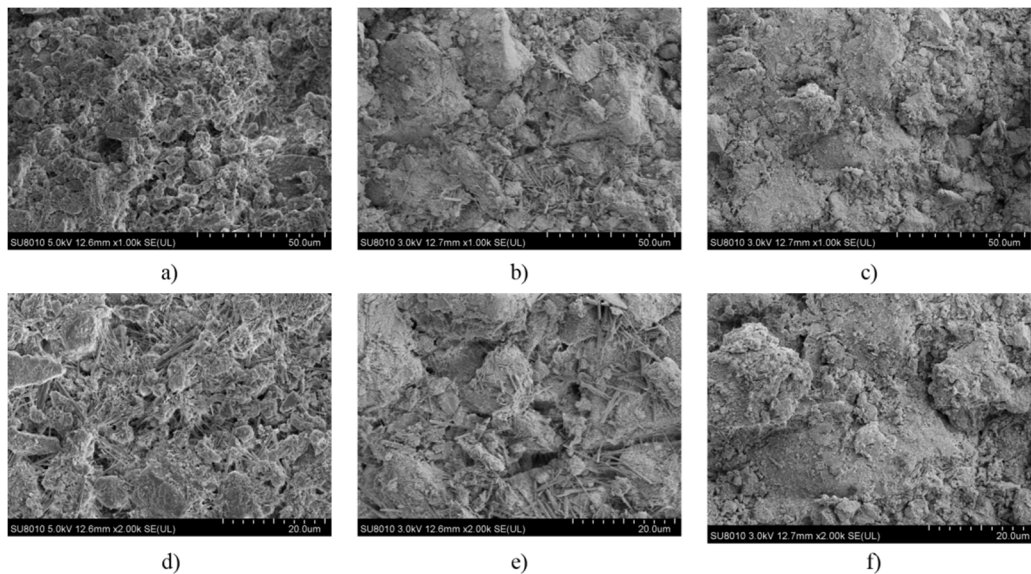


Figure 6. Electron microscope image of cement

Figure notes: a) Standing ($\times 1000$); b) Vibration 20 Hz ($\times 1000$); c) Vibration 40 Hz ($\times 1000$); d) Standing ($\times 2000$); e) Vibration 20 Hz ($\times 2000$); f) Vibration 40 Hz ($\times 2000$);

It can be observed from the microscopic morphology diagrams of 1000x and 2000x magnification that the vibration can induce the hydration products to pile up more closely, and the structure of the cement matrix shows higher continuity, and there are almost no obvious voids between the crystals. With the increase of vibration frequency, the pore size in the cement stone was gradually reduced, and the overall stacking structure was more dense, but local structural damage and peeling phenomenon also occurred. In contrast, more microcracks could be observed inside the cement stone without vibration treatment (static curing). These micro-cracks are common defects caused by the inconsistent shrinkage of each component during the hardening process of cement paste. Compared with the morphology of the control cement stone which was not subjected to vibration during the

setting period, the quiescent control group showed more micro-cracks inside the cement stone, and at the same time, in the quiescent samples, the surfaces of the stacked plate crystals were adhered to a larger number of reticulation or “cotton wool”, indicating that the hydration products were more compact. At the same time, in the static sample, there are more net-like or “cotton wool”-like hydration products attached on the surface of stacked plate-like crystals, which indicates that the distribution of hydration products is uneven, and the local accumulation of them is in the form of flocs, which fails to fill up the pores completely.

From the perspective of crystal structure, the application of simple harmonic vibration during the maintenance period can help accelerate the hydration reaction of cement. The vibration makes the cement particles and water come into contact with each other more uniformly, and provides stirring to promote the dissolution reaction, thus shortening the induced period of cement hydration and allowing more cement to hydrate rapidly. This reduces the likelihood of voids being formed by unhydrated cement and excess moisture.

In vibration-treated cement stone, the main hydration product of cement, C-S-H (calcium silicate hydrate) gel, is distributed in layers, which are gradually deposited and grown along the pore walls and crystal surfaces, and eventually fused to form a homogeneous and continuous monolithic structure. The lamellar growth of the C-S-H gel fills the void space that previously existed within the cement stone, cementing the crystal particles together and making the microstructure more integrated. In contrast, C-S-H generated under static conditions tends to be attached in the form of flocs and clusters, making it difficult to fill the pores adequately. Vibration overcomes the phenomenon of localized accumulation of hydration products by inducing uniform nucleation and growth of C-S-H within the entire matrix. Thanks to the more uniform distribution of the hydration products, the overall pore structure of the vibrated cement stone is much finer, and the porosity and capillary content are greatly reduced. The uniform filling of hydration products converts large pores into small pores or even fills them completely, which significantly improves the internal densification of the cement stone. This dense and homogeneous microstructure contributes to the strength and durability of the material.

3.2. Mercuric Pressure

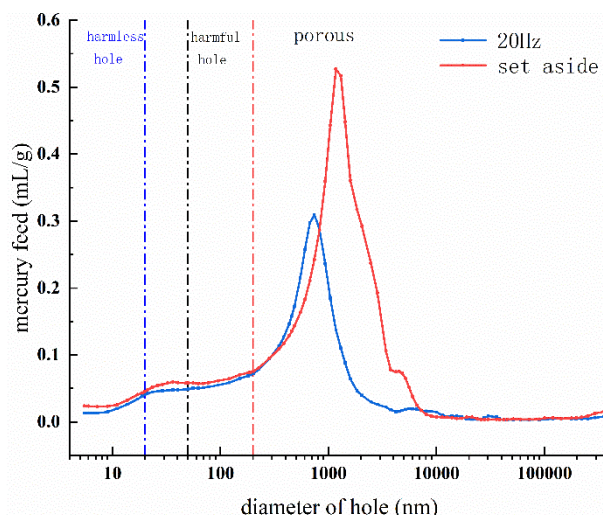


Figure 7. Pore Size Distribution by Mercury Intrusion Porosimetry

According to academician Wu Zhongwei's classification method of pore size, the pore size less than 20nm is harmless pore, the pore size from 20nm~ 50nm is less harmful pore, the pore size from 50nm~ 200nm is harmful pore, and the pore size above 200nm is more harmful pore. As can be seen in Figure 412, the unvibrated specimen in the original state, you can see the curve of the pores are mainly distributed in the 1100-1300nm, in the range of 0-100nm level there is also a small peak for

36.2nm less harmful pores, vibration frequency of 20Hz, vibration amplitude of 1mm, the vibration time of 30min vibration, the pores of the cement specimen are mainly distributed in the 600-800nm range, 0-100nm is less harmful pores, more than 200nm is more harmful pores. 800nm, the peak between 0-100nm is 23.4nm less harmful holes, the unvibrated group and vibration group relative to each other, it can be seen that the unvibrated group overall increment into the amount of mercury is higher, which explains the unvibrated group of the number of different pore sizes are higher than the vibration group. Vibration can effectively reduce the number of harmful pores and make the pores smaller within the G-grade cement stone by vibration.

3.3. Low-field Nuclear Magnetic Resonance (NMR)

(1) Porosity

Cement sample blocks can be dried and processed, and the NMR and gravimetric methods can be used. The porosity of G-grade cement stone can be obtained by testing and calculating using NMR and a precision electronic balance.

$$P = \frac{m_0 - m_1}{V} \times 100\% \quad (1)$$

P-porosity of G-grade cement sample block;

m_0 -the mass of G-grade cement sample block after vacuum water saturation;

m_1 -mass of G-grade cement sample block after vacuum saturation;

V-volume of cement sample block;

Table 4. The Effect of Vibration Frequency on Porosity

vibration frequency(Hz)	0Hz	40Hz	60Hz
porosity(%)	50.6%	30.5%	24.9%

From the porosity can be seen in the absence of vibration, the porosity obtained by NMR method and piezomercury method were 50.6%, 51.29%, respectively, to verify the correctness and reliability of the piezomercury method test, considering the piezomercury method to get the porosity corresponding to the vibration frequency of 20Hz 38.89%, the porosity of the vibration of 20Hz, 40Hz and 60Hz compared with the porosity of the static cement were reduced respectively by 23.14%, 39.72% and 50.79%, which is similar to the law of vibration frequency effect on compressive strength, and the rate of increase in compressive strength and decrease in porosity at vibration 20Hz is the most obvious compared to other vibration frequencies.

(2) Pore size distribution

The pore size distribution of cement samples can also be obtained by NMR. At the microscopic level, the magnetic resonance effect leads to a macroscopic longitudinal magnetization vector shift. Subsequently, longitudinal and transverse relaxation phenomena occur successively. Under the action of the RF pulse, the phase of some nuclei changes and absorbs energy to realize the jump to higher energy levels, and after the RF pulse stops the excitation, the phase and energy states of these nuclei will return to the initial state of excitation, which is defined as the relaxation process. The relaxation time is generally categorized into longitudinal relaxation time (T1) and transverse relaxation time (T2), and T1 reflects less information compared to T2, so generally transverse relaxation is widely used to study the aperture distribution of the sample block.

The transverse relaxation phenomenon is affected by three kinds of relaxation, namely diffusion relaxation (T2D), free relaxation (T2B) and surface relaxation (T2S), which are expressed as follows

$$\frac{1}{T_2} = \frac{1}{T_{2B}} + \frac{1}{T_{2S}} + \frac{1}{T_{2D}} \quad (2)$$

From the mercury pressure method, it can be seen that the pore scale of G-grade cementite is in the nanometer scale, so the surface relaxation plays a major role and is related to the cement pore specific surface; the free relaxation is the intrinsic relaxation property; the diffusive relaxation is due to the self-diffusive motion of the hydrogen-containing molecules in a gradient magnetic field, and the effect of the diffusive relaxation is minimized in this experiment so that the T2D can be negligible, and (2) can also be expressed as follows.

$$\frac{1}{T_2} = \frac{1}{T_{2B}} + \rho_2 \frac{S}{V} \quad (3)$$

Where ρ_2 is the surface relaxation degree and S is the surface area of cementite pores;

The relationship between NMR T2 distribution and pore size distribution is obtained by using different mathematical methods and means to get the conversion coefficients between the two to get the relationship between the pore size distribution of cementite, and the pore shape factor Fs is introduced, and the conversion can be obtained to get the pore half-price of cementite r is

$$r = \rho_2 F_s T_2 \quad (4)$$

From the formula, it can be seen that the conversion of NMR T2 distribution needs to determine the Fs and surface relaxation coefficient, it is generally believed that the pore shape of cementite is roar, $F_s = 2$, the surface relaxation of the material depends on the surface relaxation time and the “thickness” of the surface layer, and the exact value of which is more difficult to obtain, and is generally obtained by using other methods. Its exact value is difficult to obtain, and is usually obtained by other calibration methods, such as Pet-rographic Image Analysis (PIA) or Mercury Impression Pressure (MIP). In this paper, the MIP calibration method was used, and the pore size distribution curves measured by Mercury Impression Pressure (MIP) were compared with the relaxation curves obtained by Nuclear Magnetic Resonance (NMR) tests to obtain the surface relaxation of G-grade cementite.

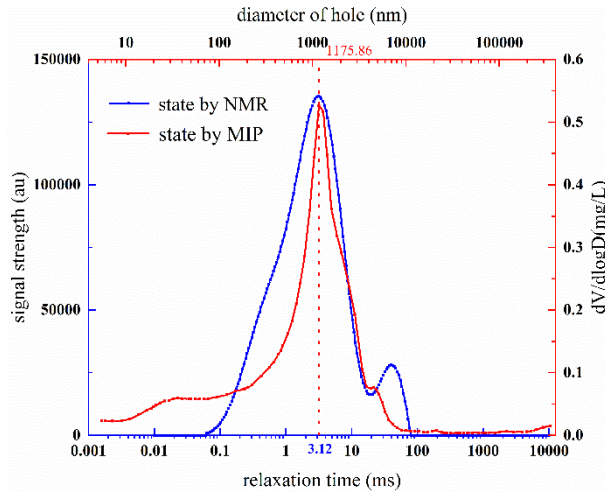


Figure 8. Comparison of Mercury Intrusion Porosimetry and Nuclear Magnetic Resonance (NMR)

From Fig. 8, it can be seen that the pore size distribution and the T2 spectrum distribution are not completely overlapped, which is due to the fact that the experiments of mercuric compression method describe more about the degree of connectivity between pore throats, and due to the complex structure of the shale pore throats, the pore-reducing throats and the short conduit-like throats are developed in large quantities, which lead to the mercury being stuck at the small throats and unable to enter into the pore, and the measured pore volume is low, and this phenomenon is known as pore shielding

effect . When NMR and MIP correspond well, the relaxation time T2 and pore size of the cementite sample are 3.12 ms and 1175.86 nm, respectively, and the relaxation coefficient ρ_2 of the G-grade cementite specimen of this experiment can be determined by substituting into Eqn. 4 as 188.43 nm/s. The distribution of pore sizes of the cementite at vibration of 40Hz and 60Hz can be obtained by utilizing 4.

Using the relaxation coefficient ρ_2 obtained above, converted to pore size can obtain the relationship between pore size and vibration frequency at higher frequencies as shown in Fig. 9 which shows that with the increase of vibration frequency, the trend is consistent with the general rule obtained by the piezoelectric mercury method, the multi-hazardous pore pore size and volume decrease, and the pore size decreases. With the increase of vibration frequency, the maximum value of pore size percentage was 1175nm, 521.62nm and 494.91nm, the vibration pore size decreased by 55.6% and 57.88%, respectively, and the signal intensity corresponding to the maximum pore size was 135306, 123506 and 80198.9, respectively, and the signal intensity decreased by 8.7% and 40.72%, respectively, which could be seen that With the increase of vibration frequency the volume of harmful pores decreases rapidly, when the vibration frequency 40Hz, more harmful pores receive the influence of vibration, and more harmful pores are affected to become harmful pores, so the volume of harmful pores increases, but when vibration is 60Hz, the volume of harmful pores also decreases again, which is the same as the vibration frequency effect on the compressive strength law. Most of the pores of cement stone are harmful pores, which is due to the cement formula is only G grade cement, without adding various external additives and external admixtures.

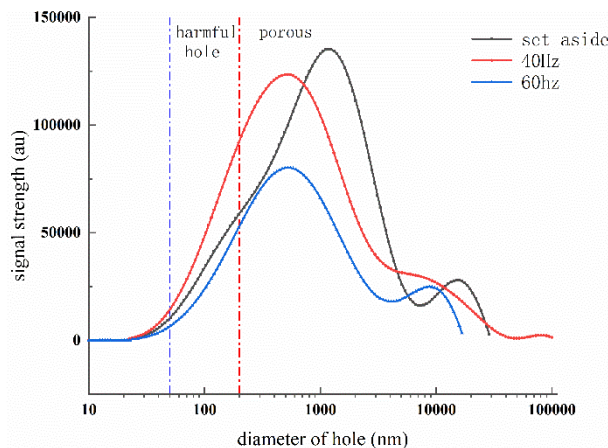


Figure 9. Pore Size Distribution by Nuclear Magnetic Resonance (NMR)

4. SUMMARY

(1) The experiment on the effect of vibration on the mechanical properties of cement stone was carried out, and the study shows that vibration can significantly improve the compressive strength and cementation strength of cement stone. Within a certain range, with the increase of vibration frequency and time, the compressive strength gradually increases, while the cementitious strength shows a trend of increasing first and then tends to stabilize, which provides theoretical support for the selection of vibration parameters.

(2) Through the equipment of electron microscope, piezoelectric mercury meter and low-field nuclear magnetic resonance analyzer, it is found that vibration can promote the cement particles to be distributed more uniformly and reduce the number and size of pores, and the vibration of 20Hz, 40Hz and 60Hz reduces the porosity of cement compared with that of static cement by 23.14%, 39.72% and 50.79%, respectively, and improves the densification degree of cement stone. The improvement of microstructure is the fundamental reason for the vibration-enhanced performance of cement stone.

(3) The experiments of pressed mercury method and nuclear magnetic resonance (NMR) method were carried out to clarify the effect of vibration frequency on porosity, determine the relaxation coefficient of G-grade cement according to the results of the pressed mercury method, and obtain the distribution of pore size under different vibration frequencies.

ACKNOWLEDGMENTS

This research was Supported by The Innovation Fund of Postgraduate, Sichuan University of Science & Engineering. (Grant No. Y2023095).

REFERENCES

- [1] HAN Yu'an, SUN Yanlong, WANG Hongchao, et al. Development status of vibratory cementing technology at home and abroad[J]. *Drilling Technology*, 2000(4): 29-32.
- [2] Ding Baogang. *Fundamentals of Cementing Technology* [M]. Petroleum Industry Press, 2006.
- [3] LI Yuhai, ZHAO Lixin, WANG Junrong. Review of vibratory cementing technology[J]. *Oil Drilling Technology*, 1994(6): 40-42+50-98.
- [4] Cooke C E, Gonzalez O J, Broussard D J. Primary Cementing Improvement by Casing Vibration During Cement Curing Time[J]. *SPE Production Engineering*, 1988, 3(03): 339-345.
- [5] Lu Y, Dai Z. Dynamics model of redundant hybrid manipulators connected in series by three or more different parallel manipulators with linear active legs[J]. *Mechanism and Machine Theory*, 2016, 103: 222-235.
- [6] Chow T W, Mcintire L V, Kunze K R, et al. The Rheological Properties of Cement Slurries: Effects of Vibration, Hydration Conditions, and Additives[J]. *SPE Production Engineering*, 1988, 3(04): 543-550.
- [7] Dusterhoft D, Wilson G, Newman K. Field study on the use of cement pulsation to control gas migration[C]//*SPE Gas Technology Symposium*. Calgary, Alberta, Canada: SPE, 2002: SPE-75689.
- [8] Li Jinfu. Development of downhole movable vibratory cementing system based on eccentric oscillator[J]. *Petroleum Mining Machinery*, 2024, 53(2): 48-56.
- [9] YIN Wenbo, ZHANG Yanting, LI Yanwei, et al. Experiment on the effect of vibration in casing of cementing shaker on the strength of cementite[J]. *Petroleum Machinery*, 2018, 46(4): 1-6.
- [10] YIN Yiyong, WANG Zhaohui, REN Xing, et al. Development of downhole screw motor bidirectional vibration cementing tool[J]. *Petroleum Machinery*, 2017, 45(1): 10-14.
- [11] Ren Xing. *Development of downhole hydraulic pulse vibration cementing device* [D]. Beijing: China University of Petroleum (Beijing), 2016.
- [12] HUANG Peng, LI Yang, LI Dong, et al. Experimental study on radial cementation strength at the first interface of high temperature and high pressure cementing[J]. *Petroleum Machinery*, 2021, 49(11): 39-44.
- [13] YANG Yuanguang, FANG Zhongqi, YUAN Bin, et al. Evaluation of the integrity of cement ring interface based on tensile bond strength[J]. *Journal of Southwest Petroleum University (Natural Science Edition)*, 2021, 43(4): 183-190.
- [14] LIU Baobo, CHEN Bin, LI Bin, et al. Study on the effect of cement type on cementation strength and sealing property of cemented well rings[J]. *Tianjin Science and Technology*, 2022, 49(1): 28-31, 34.